

Space Domain based Ecological Cooperative and Adaptive Cruise Control on Rolling Terrain

Mingyue Lei

Research Assistant

Key Laboratory of Road and Traffic Engineering of the Ministry of Education, Tongji
University, 4800 Cao'an Road, Shanghai, P.R.China

Department of Civil and Environmental Engineering, University of California, Los
Angeles, CA 90024 USA

Email: mingyue2024@g.ucla.edu

Haoran Wang, Ph.D., Corresponding Author

Associate Researcher

Key Laboratory of Road and Traffic Engineering of the Ministry of Education, Tongji
University, 4800 Cao'an Road, Shanghai, P.R.China

State Key Laboratory of Advanced Design and Manufacturing for Vehicle Body, Hunan
University, Changsha, 410082, China

Email: wang_haoran@tongji.edu.cn

Duo Li, Ph.D.

Senior Lecturer (Associate Professor)

Department of Civil and Geospatial Engineering

Newcastle University

Newcastle upon Tyne NE1 7RU, UK

Email: Duo.li@newcastle.ac.uk

Zhenning Li, Ph.D.

Assistant Professor

State Key Laboratory of Internet of Things for Smart City

Departments of Civil and Environmental Engineering and Computer and Information
Science

University of Macau

Avenida da Universidade Taipa, Macau, China

Email: zhenningli@um.edu.mo

Ashish Dhamaniya, Ph.D.

Associate Professor

Head - Transportation Engineering & Planning Section

Department of Civil Engineering

SV National Institute of Technology

Surat-395007, Gujarat, India

Email: adhamaniya@gmail.com

Jia Hu, Ph.D.

ZhongTe Distinguished Chair in Cooperative Automation, Professor

Key Laboratory of Road and Traffic Engineering of the Ministry of Education

Institute for Advanced Study

Tongji University

4800 Cao'an Road, Shanghai, P.R.China

Email: hujia@tongji.edu.cn

Abstract

Ecological Cooperative and Adaptive Cruise Control (Eco-CACC) is widely focused to enhance sustainability of CACC. However, state-of-the-art Eco-CACC studies are still facing challenges in adopting on rolling terrain. Furthermore, they cannot ensure both ecology optimality and computational efficiency. Hence, this paper proposes a nonlinear optimal control based Eco-CACC controller. It has the following features: i) enhancing performance across rolling terrains by modeling in space domain; ii) enhancing fuel efficiency via globally optimizing all vehicle's fuel consumptions; iii) ensuring computational efficiency by developing a differential dynamic programming-based solving method for the non-linear optimal control problem; iv) ensuring string stability through theoretically proving and experimentally validating. The performance of the proposed Eco-CACC controller was evaluated. Results showed that the proposed Eco-CACC controller can improve average fuel saving by 37.67% at collector road and about 17.30% at major arterial.

Keywords: Cooperative and Adaptive Cruise Control; Ecological driving; Rolling terrain; Spatial domain; Nonlinear optimal control; String stability

Declarations of interest: none

I. INTRODUCTION

Cooperative and Adaptive Cruise Control (CACC) technology emerges as an advancement over Adaptive Cruise Control (ACC) technology (Turri V et al., 2016; Sakhdari B et al., 2017; Zhang Y et al., 2020; Wang H et al., 2022; Kazemi H et al., 2018). It enables a platoon to maintain a reduced inter-vehicular distance without vehicle speed fluctuations. This capability contributes to diminishing the aerodynamic resistance for the

platoon, which has the potential to reduce energy consumptions and emissions. Building upon this, Ecological CACC (Eco-CACC) is introduced with the objectives of enhancing fuel efficiency through the utilization of CACC technology.

However, existing Eco-CACC researches are still with limitations.

Firstly, most of existing Eco-CACC researches lack adaptability in driving on rolling terrain, which is common in road transportation. These researches do not take road slope into consideration, so it turns out that adopting the same control policy on different slopes (Rezaee H et al., 2023; Wang Z et al., 2017; Ma H et al., 2020; Han S Y et al., 2013; Wang Z et al., 2018; Zhang Y et al., 2022). However, these policies result in wasted power and enhanced fuel consumption. It is due to that vehicles on different slopes experience different frictional forces and horizontal components of gravity. To follow the constant control policy, the engine of the vehicle is inevitably engaged in compensating for resistance on uphill and idling on downhill. Excessive fuel is consumed without contributing to productive work. Hence, vehicles should be provided with dynamic power, that is related to the road slopes at their positions. Some researches adopt this strategy and introduce road slope into the control system as an external disturbance (Li J et al., 2023; Turri V et al., 2018; Zhai C et al., 2018). However, this design leads to computational inefficiency. The reason is that the disturbance is a variant value relative to system state, increasing the dimension of the model. Therefore, it is necessary to develop a controller that both considering road slope and avoiding reducing adaptability.

Secondly, the fuel-saving benefits for the entire platoon still have room for improvement. For most of the existing Eco-CACC researches (Duan H et al., 2022; Lin Y C et al., 2019; Luu D L et al., 2021), only the platoon leader's ecology efficiency is optimized. The

followers just track the leader's speed as the reference. This design is incapable to optimally save the followers' fuel consumption, as each vehicle within the platoon has its individual vehicle dynamics and road conditions it encounters. Hence, in order to achieve greater fuel efficiency, it is necessary to develop a centralized system which could optimize all the platoon vehicles' fuel consumption simultaneously.

Thirdly, the solutions in existing Eco-CACC researches face challenges in ensuring both optimality and computational efficiency. The problem of energy optimization for multiple vehicles tends to be modelled as a non-convex and non-linear formulation. Many researches utilize heuristic algorithms to resolve it (Zhai C et al., 2018; Ma H et al., 2020; Liu B et al., 2015). Heuristic algorithms cannot always guarantee optimal solutions, and the speed of convergence is unstable. There are also some researches dividing the formulation into sub-problems, and utilizing layered optimization methods to derive a solution (Murgovski N et al., 2016). This strategy also sacrifices precision for computation efficiency, impeding the performance of Eco-CACC applications. Hence, there is a significant demand for a solution method that ensures both optimality and computational efficiency.

To address the above deficiencies, this paper proposes an advanced Eco-CACC system that is fine-tuned for the following capabilities:

- **Superior performance across rolling terrains:** designing a controller modelled in space domain to keep the road slope constant.
- **Enhanced fuel efficiency:** leveraging a centralized approach to optimize each vehicle's fuel efficiency within the platoon.

- **Real-time applicability with assured optimality:** developing a differential dynamic programming-based method that rapidly provides the optimal solution to non-linear optimal control problems.
- **Sting stability ensured:** mathematically analyzing and proving the string stability of the proposed Eco-CACC controller.

This paper is organized as follows: Section II provides detailed formulations about the proposed system. Section III reveals the solution to the Eco-CACC controller in the system. Section IV provides the string stability analysis of the controller. Section V demonstrates the experiment design and evaluation analysis. Section VI provides discussions. Section VII presents conclusions.

II. PROBLEM FORMULATION

A. Overall Architecture

The architecture of the proposed Eco-CACC system is depicted in Figure 1. It adopts a bifurcated structure consisting of an upper-centralized planning level and a lower-distributed actuation level. This paper focuses on the upper-centralized planning. The architecture is demonstrated as follows:

The upper-centralized planning is achieved by the proposed Eco-CACC controller. It integrates both roadside and vehicular information to formulate optimal acceleration commands for each vehicle within the platoon. Parameters such as expected speed and inter-vehicle time spacing are pre-configured within this central controller to guide the platooning behavior.

The lower-distributed actuating is achieved by the individual vehicle's actuator. These actuators are assumed to be already equipped on the automated vehicle. They are capable of real-time executing commands from the proposed Eco-CACC controller.

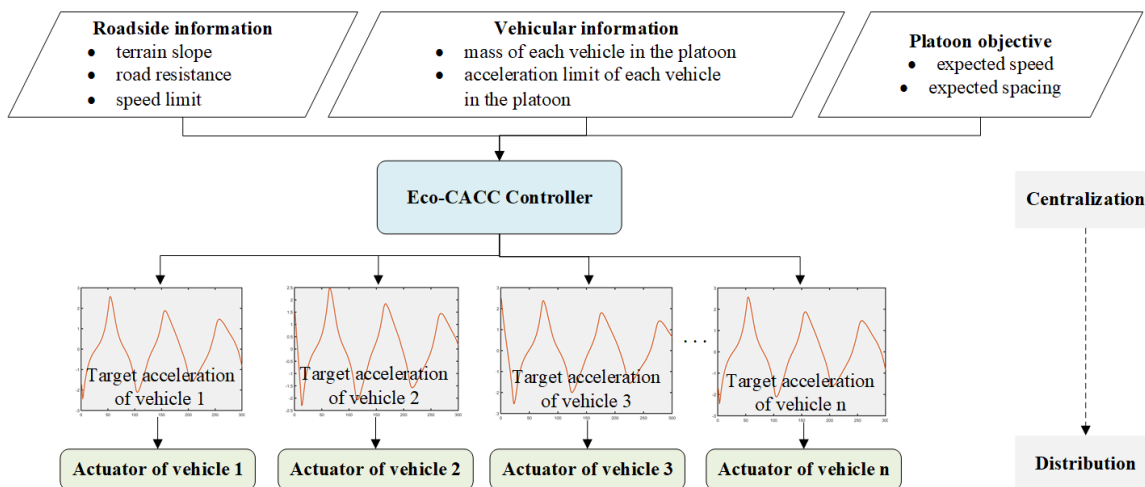


Figure 1. Architecture of the proposed centralization-distribution Eco-CACC system.

B. Space Domain based Eco-CACC Controller

The formulation of the proposed Eco-CACC controller is presented.

1) State explanation

Definition 1 (Slowness): Slowness is the time a vehicle takes to travel through a unit distance:

$$\pi \stackrel{\text{def}}{=} \frac{dt}{ds} = \frac{1}{v} \quad (1)$$

The system state vector \mathbf{X} is as follows:

$$\mathbf{X}_k \quad (2)$$

$$\begin{aligned}
&= [t_{1,k} - t_{2,k} - h, \pi_{1,k} - \pi_{2,k}, \dots, t_{1,k} - t_{i,k} - (i-1)h, \pi_{1,k} \\
&\quad - \pi_{i,k}, \dots, t_{1,k} - t_{N,k} - (N-1)h, \pi_{1,k} \\
&\quad - \pi_{N,k}]^T, i \in [2, N], k \in [0, K] \\
&\pi_{i,k} = \frac{1}{v_{i,k}}, i \in [1, N], k \in [0, K]
\end{aligned} \tag{3}$$

where $t_{i,k}$ is the arriving time of the i^{th} vehicle in the platoon at step k , $\pi_{i,k}$ is the slowness of the i^{th} vehicle in the platoon at step k , $v_{i,k}$ is the speed of the i^{th} vehicle in the platoon at step k , N is the number of vehicles in the platoon, h is the expected time headway between adjacent vehicles in the platoon, K is the control horizon.

The control vector \mathbf{U} is defined as follows:

$$\mathbf{U}_k = [a_{1,k}, \dots, a_{i,k}, \dots, a_{N,k}]^T, i \in [1, N], k \in [0, K-1] \tag{4}$$

where $a_{i,k}$ is the acceleration of the i^{th} vehicle in the platoon at step k .

2) System dynamics

The dynamics of vehicles is formulated based on a nonlinear bicycle model (R. Rajamani, 2011). The dynamics is described as follows:

$$\begin{aligned}
&\mathbf{X}_{k+1} \\
&= (\mathbf{A} \cdot \Delta s + \mathbf{I}_{2(N-1) \times 2(N-1)}) \mathbf{X}_k + (\mathbf{B}_k \cdot \Delta s) \mathbf{U}_k, k \in [0, K-1]
\end{aligned} \tag{5}$$

with

$$\mathbf{A} = \begin{bmatrix} \mathbb{A} & \mathbf{0} & \cdots & \mathbf{0} \\ \mathbf{0} & \mathbb{A} & \cdots & \mathbf{0} \\ \vdots & \vdots & \ddots & \vdots \\ \mathbf{0} & \mathbf{0} & \cdots & \mathbb{A} \end{bmatrix}_{2(N-1) \times 2(N-1)} \quad (6)$$

$$\mathbb{A} = \begin{bmatrix} 0 & 1 \\ 0 & 0 \end{bmatrix} \quad (7)$$

$$\mathbf{B}_k = \begin{bmatrix} \mathbb{B}_k^1 & \mathbb{B}_{2,k}^2 & \cdots & \mathbf{0} \\ \vdots & \vdots & \ddots & \vdots \\ \mathbb{B}_k^1 & \mathbf{0} & \cdots & \mathbb{B}_{N,k}^2 \end{bmatrix}_{2(N-1) \times N}, k \in [0, K-1] \quad (8)$$

$$\mathbb{B}_k^1 = \begin{bmatrix} 0 \\ -(\pi_{1,k})^3 \end{bmatrix}, k \in [0, K-1] \quad (9)$$

$$\mathbb{B}_{i,k}^2 = \begin{bmatrix} 0 \\ (\pi_{i,k})^3 \end{bmatrix}, i \in [2, N], k \in [0, K-1] \quad (10)$$

where \mathbf{A} is the state coefficient matrix, \mathbb{A} is the unit block of the diagonal coefficient matrix \mathbf{A} , Δs is the space increment in each step, \mathbf{B}_k is the control coefficient matrix at step k , \mathbb{B}_k^1 and $\mathbb{B}_{i,k}^2$ are the unit blocks of the diagonal coefficient matrix \mathbf{B}_k .

3) Cost function

$$J = \sum_{i=0}^{K-1} L(\mathbf{X}_i, \mathbf{U}_i) + l^f(\mathbf{X}_K) \quad (11)$$

with

$$\begin{aligned} & L(\mathbf{X}_k, \mathbf{U}_k) \\ &= \sum_{i=2}^N q_1 (t_{1,k} - t_{i,k} - (i-1)h)^2 \end{aligned} \quad (12)$$

$$\begin{aligned}
& + \sum_{i=1}^N q_2 (m_i a_{i,k} v_{i,k} + m_i g \sin(\theta_k) v_{i,k} + \mu m_i g \cos(\theta_k) v_{i,k} \\
& \quad + \xi v_{i,k}^3) \\
& \quad + \sum_{i=1}^N r_1 a_{i,k}^2, k \in [0, K-1] \\
l^f(\mathbf{X}_K) & = \sum_{i=1}^N q_3 \left(t_{i,K} - \frac{K \cdot \Delta s}{v^d} \right)^2 \tag{13}
\end{aligned}$$

where $L(\mathbf{X}, \mathbf{U})$ is the running cost function, $l^f(\mathbf{X})$ is the terminal cost function, q_1 , q_2 , q_3 and r_1 are non-negative weighting parameters, m_i is the mass of the i^{th} vehicle in the platoon, g is gravity, θ_k is the terrain slope at step k , which is constant relative to longitudinal position (control step). μ is a constant describing the rolling resistance, ξ is a constant describing drag, v^d is the target average speed. $\sum_{i=2}^N q_1 (t_{1,k} - t_{i,k} - (i-1)h)^2$ is a CACC cost. The CACC cost is designed to maintain a desired time gap between adjacent vehicles in the platoon. $\sum_{i=1}^N q_2 (m_i a_{i,k} v_{i,k} + m_i g \sin(\theta_k) v_{i,k} + \mu m_i g \cos(\theta_k) v_{i,k} + \xi v_{i,k}^3)$ is an ecology cost. The ecology cost is designed to reduce total fuel consumption of the platoon. The terminal cost is designed to guarantee the mobility of the platoon.

4) Boundary conditions

The initial system state is a boundary condition, which is obtained via V2I communication:

$$\mathbf{X}_0 \tag{14}$$

$$= [t_{1,0} - t_{2,0} - h, \pi_{1,0} - \pi_{2,0}, \dots, t_{1,0} - t_{i,0} - (i-1)h, \pi_{1,0} - \pi_{i,0}, \dots, t_{1,0} - t_{N,0} - (N-1)h, \pi_{1,0} - \pi_{N,0}]^T, i \in [2, N]$$

where $t_{i,0}$ is the moment that the i^{th} vehicle in the platoon reaches the starting position, $\pi_{i,0}$ is the slowness of the i^{th} vehicle in the platoon at the starting position.

5) Constraints

(a) Speed limit

Considering the speed limit, vehicle speed should be limited within the range:

$$0 \leq v_{i,k} \leq v_{max}, i \in [1, N], k \in [0, K] \quad (15)$$

where v_{max} is the speed limit.

(b) Acceleration limit

Each vehicle's acceleration should be limited considering the individual vehicle's capability:

$$a_{i,min} \leq a_{i,k} \leq a_{i,max}, i \in [1, N], k \in [0, K-1] \quad (16)$$

where $a_{i,min}$ is the minimum acceleration of the i^{th} vehicle in the platoon, and $a_{i,max}$ is the maximum acceleration of the i^{th} vehicle in the platoon.

III. PROBLEM SOLVING

The proposed Eco-CACC controller is a non-linear optimal controller. To ensure computational efficiency, a differential dynamic programming-based method is proposed in this section. The detailed process is as follows.

A. Step 1: Modelling the Optimal Cost-to-go Function

In an optimal control problem, the optimality of future control actions is independent of historical control or state trajectories. Consequently, the optimal cost-to-go function is constructed to reflect the minimum achievable cost from a given state, encapsulating the essence of optimality in this context.

To incorporate constraints within the optimization framework, the Augmented Lagrangian Method is employed. This approach serves to reformulate the cost function in equation (12), enabling a more comprehensive solution to the control problem.

$$J^P = \sum_{i=0}^{K-1} L^P(\mathbf{X}_i, \mathbf{U}_i) + l^f(\mathbf{X}_K) \quad (17)$$

with

$$\begin{aligned} & L^P(\mathbf{X}_k, \mathbf{U}_k) \\ &= L(\mathbf{X}_k, \mathbf{U}_k) + \frac{1}{2} \sum_{i=1}^{\varepsilon} C_i(\mathbf{X}_k, \mathbf{U}_k)^T \rho_i C_i(\mathbf{X}_k, \mathbf{U}_k) \\ & \quad + \sum_{i=1}^{\varepsilon} \lambda_i C_i(\mathbf{X}_k, \mathbf{U}_k), k \in [0, K-1] \end{aligned} \quad (18)$$

$$C_i(\mathbf{X}_k, \mathbf{U}_k) = c_i(\mathbf{X}_k, \mathbf{U}_k) + s_i, i \in [1, \varepsilon], k \in [0, K-1] \quad (19)$$

where $L^P(\mathbf{X}, \mathbf{U})$ is the running cost function containing the penalty of constraint violations, $C_i(\mathbf{X}, \mathbf{U})$ is the i^{th} equality constraint, ε is the number of equality constraints. According to equation (15) and equation (16), for each vehicle in the platoon, there exist four constraints to be set. Hence, ε equals to $4 * N$ in this research. ρ_i is a scale weighting parameter for the i^{th} equality constraint violation, λ_i is the Lagrange multiplier for the i^{th} equality constraint. The update for λ_i shall be presented in the equation (45). $c_i(\mathbf{X}, \mathbf{U})$ is the i^{th} inequality constraint, which can be derived from equation (15) and equation (16). s_i is the slacking variable for the i^{th} inequality constraint. The update for s_i is presented in the equation (44).

According to the cost function equation (17), the optimal cost-to-go function at step k is defined as follows.

$$V_k(\mathbf{X}) = \min_{\mathbf{u}} \sum_{i=k}^{K-1} L^P(\mathbf{X}_i, \mathbf{U}_i) + l^f(\mathbf{X}_K), k \in [0, K-1] \quad (20)$$

where $\mathbf{u} = \{\mathbf{U}_k, \mathbf{U}_{k+1}, \dots, \mathbf{U}_{K-1}\}$ is a sequence of control.

Using Bellman's principle of optimality (R. Bellman, 1966; S. Wright et al., 1999), the optimal cost-to-go function can be rewritten in a recursive formulation.

$$V_k(\mathbf{X}) = \min_{\mathbf{U}_k} L^P(\mathbf{X}_k, \mathbf{U}_k) + V_{k+1}(\mathbf{f}(\mathbf{X}_k, \mathbf{U}_k)), k \in [0, K-1] \quad (21)$$

where \mathbf{f} is the dynamics function that governs the state transition given the current state and control. The formulation of \mathbf{f} can be derived from equation (5) to equation (9).

The boundary condition is:

$$V_K(\mathbf{X}) = l^f(\mathbf{X}_K) \quad (22)$$

Considering the minimization problem in equation (21) is non-linear, local approximation to the optimal cost-to-go function is introduced to settle the computational difficulty caused by nonlinearity.

Local change in the minimization argument in equation (21) under perturbation $(\boldsymbol{\delta}_X, \boldsymbol{\delta}_U)$ is:

$$\begin{aligned} & Q_k(\boldsymbol{\delta}_X, \boldsymbol{\delta}_U) \\ &= L^P(\mathbf{X}_k + \boldsymbol{\delta}_X, \mathbf{U}_k + \boldsymbol{\delta}_U) \\ &+ V_{k+1}(\mathbf{f}(\mathbf{X}_k + \boldsymbol{\delta}_X, \mathbf{U}_k + \boldsymbol{\delta}_U)), k \in [0, K-1] \end{aligned} \quad (23)$$

For the convenience of recursive iteration, $Q_k(\boldsymbol{\delta}_X, \boldsymbol{\delta}_U)$ is expanded by second-order Taylor about $(\mathbf{0}, \mathbf{0})$:

$$\begin{aligned} & Q_k(\boldsymbol{\delta}_X, \boldsymbol{\delta}_U) \\ & \approx \frac{1}{2} \begin{bmatrix} \mathbf{1} \\ \boldsymbol{\delta}_X \\ \boldsymbol{\delta}_U \end{bmatrix}^T \begin{bmatrix} \mathbf{0} & \mathbf{Q}_{X,k}^T & \mathbf{Q}_{U,k}^T \\ \mathbf{Q}_{X,k} & \mathbf{Q}_{XX,k} & \mathbf{Q}_{XU,k} \\ \mathbf{Q}_{U,k} & \mathbf{Q}_{XU,k}^T & \mathbf{Q}_{UU,k} \end{bmatrix} \begin{bmatrix} \mathbf{1} \\ \boldsymbol{\delta}_X \\ \boldsymbol{\delta}_U \end{bmatrix}, k \in [0, K-1] \end{aligned} \quad (24)$$

where the block matrices are computed as:

$$\mathbf{Q}_{X,k} = L_{X,k}^P + \mathbf{f}_{X,k}^T \mathbf{b}_{k+1} \quad (25)$$

$$\mathbf{Q}_{U,k} = L_{U,k}^P + \mathbf{f}_{U,k}^T \mathbf{b}_{k+1} \quad (26)$$

$$\mathbf{Q}_{XX,k} = L_{XX,k}^P + \mathbf{f}_{X,k}^T \mathbf{A}_{k+1} \mathbf{f}_{X,k} + \mathbf{b}_{k+1}^T \mathbf{f}_{XX,k} \quad (27)$$

$$\mathbf{Q}_{UU,k} = L_{UU,k}^P + \mathbf{f}_U^T \mathbf{A}_{k+1} \mathbf{f}_U + \mathbf{b}_{k+1}^T \mathbf{f}_{UU} \quad (28)$$

$$\mathbf{Q}_{UX,k} = L_{UX,k}^P + \mathbf{f}_U^T \mathbf{A}_{k+1} \mathbf{f}_X + \mathbf{b}_{k+1}^T \mathbf{f}_{UX} \quad (29)$$

$$L_{\mathbf{X},k}^P = L_{\mathbf{X},k} + \sum_{i=1}^{\varepsilon} c_{i\mathbf{X}}^T \lambda_i + \sum_{i=1}^{\varepsilon} c_{i\mathbf{X}}^T \rho_i (c_i + s_i) \quad (30)$$

$$L_{\mathbf{U},k}^P = L_{\mathbf{U},k} + \sum_{i=1}^{\varepsilon} c_{i\mathbf{U}}^T \lambda_i + \sum_{i=1}^{\varepsilon} c_{i\mathbf{U}}^T \rho_i (c_i + s_i) \quad (31)$$

$$L_{\mathbf{X}\mathbf{X},k}^P = L_{\mathbf{X}\mathbf{X},k} + \sum_{i=1}^{\varepsilon} c_{i\mathbf{X}}^T \rho_i c_{i\mathbf{X}} \quad (32)$$

$$L_{\mathbf{U}\mathbf{U},k}^P = L_{\mathbf{U}\mathbf{U},k} + \sum_{i=1}^{\varepsilon} c_{i\mathbf{U}}^T \rho_i c_{i\mathbf{U}} \quad (33)$$

$$\begin{aligned} & L_{\mathbf{U}\mathbf{X},k}^P \\ &= L_{\mathbf{U}\mathbf{X},k} + \sum_{i=1}^{\varepsilon} \lambda_i^T c_{i\mathbf{U}\mathbf{X}} + \sum_{i=1}^{\varepsilon} c_{i\mathbf{U}\mathbf{X}}^T \rho_i (c_i + s_i) \\ & \quad + \sum_{i=1}^{\varepsilon} c_{i\mathbf{U}}^T \rho_i c_{i\mathbf{X}} \end{aligned} \quad (34)$$

where \mathbf{b}_{k+1} is the gradient of $V_{k+1}(\mathbf{X})$, \mathbf{A}_{k+1} is the Hessian of $V_{k+1}(\mathbf{X})$.

B. Step 2: Computing the Control Law

In order to solve the optimization in the optimal cost-to-go function, $Q_k(\boldsymbol{\delta}_{\mathbf{X}}, \boldsymbol{\delta}_{\mathbf{U}})$ in the equation (24) is minimized with respect to $\boldsymbol{\delta}_{\mathbf{U}}$. The linear feedback control law is then computed:

$$\boldsymbol{\delta}_U = \mathbf{h}_k \boldsymbol{\delta}_X + \mathbf{j}_k, k \in [0, K - 1] \quad (35)$$

with

$$\mathbf{h}_k = -\mathbf{Q}_{UU,k}^{-1} \mathbf{Q}_{UX,k}^T \quad (36)$$

$$\mathbf{j}_k = -\mathbf{Q}_{UU,k}^{-1} \mathbf{Q}_{U,k}^T \quad (37)$$

C. Step 3: Updating the Optimal Cost-to-go Function

In order to calculate the optimal control law evaluated at \mathbf{X}_k recursively, the optimal cost-to-go function evaluated at \mathbf{X}_k needs to be obtained according to the equation (21). By substituting the equation (35) into the equation (24) and equation (23), $V_k(\mathbf{X})$ is updated:

$$\begin{aligned} & V_k(\mathbf{X}) \\ &= \frac{1}{2} (\mathbf{X} - \mathbf{X}_k)^T \mathbf{A}_k (\mathbf{X} - \mathbf{X}_k) + \mathbf{b}_k^T (\mathbf{X} - \mathbf{X}_k) \\ & \quad + c_k, k \in [0, K - 1] \end{aligned} \quad (38)$$

with

$$\mathbf{A}_k = \mathbf{Q}_{XX,k} + \mathbf{h}_k^T \mathbf{Q}_{UU,k} \mathbf{h}_k + \mathbf{Q}_{UX,k}^T \mathbf{h}_k + \mathbf{h}_k^T \mathbf{Q}_{UX,k} \quad (39)$$

$$\mathbf{b}_k = \mathbf{Q}_{X,k} + \mathbf{h}_k^T \mathbf{Q}_{UU,k} \mathbf{j}_k + \mathbf{Q}_{UX,k}^T \mathbf{j}_k + \mathbf{h}_k^T \mathbf{Q}_{U,k} \quad (40)$$

$$c_k = \frac{1}{2} \mathbf{j}_k^T \mathbf{Q}_{UU,k} \mathbf{j}_k + \mathbf{j}_k^T \mathbf{Q}_{U,k} + Q_k(\mathbf{0}, \mathbf{0}) \quad (41)$$

where c_k is the constant term irrelevant to the solution. \mathbf{b}_k and \mathbf{A}_k evaluated at \mathbf{X}_k shall be passed to the previous step $k - 1$. Starting with $\mathbf{A}_K = l^f_{\mathbf{X}\mathbf{X}}$ and $\mathbf{b}_K = l^f_{\mathbf{X}}, \mathbf{h}_k, \mathbf{j}_k, \mathbf{A}_k, \mathbf{b}_k$ can be recursively solved from step K to step 0.

D. Step 4: Updating State Trajectory

A new state trajectory is updated applying the above optimal control law. The update is forward passed starting with $\mathbf{X}_0^{new} = \mathbf{X}_0$.

$$\mathbf{U}_k^{new} = \mathbf{U}_k + \mathbf{h}_k(\mathbf{X}_k^{new} - \mathbf{X}_k) + \mathbf{j}_k, k \in [0, K - 1] \quad (42)$$

$$\mathbf{X}_{k+1}^{new} = \mathbf{f}(\mathbf{X}_k^{new}, \mathbf{U}_k^{new}), k \in [0, K - 1] \quad (43)$$

E. Step 5: Updating Lagrange Multipliers and Slacking Variables

After updating state trajectory, s_i and λ_i are updated for improved approximation of \mathbf{X}_k^* at the next iteration.

$$s_i = -\rho_i^{-1}\lambda_i - c_i, i \in [1, \varepsilon] \quad (44)$$

$$\lambda_i = \lambda_i + c_i + s_i, i \in [1, \varepsilon] \quad (45)$$

Repeatedly performing the backward (Step 1 to Step 3) - forward (Step 4 to Step 5) process, the algorithm shall converge within a specified tolerance and the optimal state trajectory sequence $[\mathbf{X}_1^*, \dots, \mathbf{X}_k^*, \dots, \mathbf{X}_K^*], k \in [0, K]$ shall be obtained.

IV. STRING STABILITY ANALYSIS

This section provides proof of string stability for the proposed platoon controller.

Optimal control law is utilized for stability analysis. Pontryagin's Minimum Principle (PMP) is introduced to calculate the optimal control law. Necessary conditions for the calculation are as follows:

$$H(\mathbf{X}, \mathbf{U}, \boldsymbol{\lambda}) = L(\mathbf{X}, \mathbf{U}) + \boldsymbol{\lambda}^T f(\mathbf{X}, \mathbf{U}) \quad (46)$$

$$H(\mathbf{X}^*, \mathbf{U}^*, \boldsymbol{\lambda}^*) \leq H(\mathbf{X}, \mathbf{U}, \boldsymbol{\lambda}) \quad (47)$$

$$-\frac{d\boldsymbol{\lambda}}{dx} = \frac{\partial H}{\partial \mathbf{X}} = \frac{\partial f}{\partial \mathbf{X}} \boldsymbol{\lambda} + \frac{\partial L}{\partial \mathbf{X}} \quad (48)$$

where H is Hamiltonian, \mathbf{X} is the system state vector, \mathbf{U} is the control vector, and $\boldsymbol{\lambda}$ is a co-state vector. $L(\mathbf{X}, \mathbf{U})$ is the cost function, $f(\mathbf{X}, \mathbf{U})$ is the system dynamics function, $\mathbf{X}^*, \mathbf{U}^*, \boldsymbol{\lambda}^*$ are the optimal solutions.

Applying equation (12):

$$L(\mathbf{X}, \mathbf{U}) = \mathbf{X}^T \mathbf{M} \mathbf{X} + \mathbf{N} \mathbf{X} + \mathbf{U}^T \mathbf{R} \mathbf{U} + \mathbf{D} \mathbf{U} + \mathbf{F} \quad (49)$$

with

$$\mathbf{M} = \begin{bmatrix} \mathbb{M} & \mathbf{0} & \dots & \mathbf{0} \\ \mathbf{0} & \mathbb{M} & \dots & \mathbf{0} \\ \vdots & \vdots & \ddots & \vdots \\ \mathbf{0} & \mathbf{0} & \dots & \mathbb{M} \end{bmatrix}_{2(N-1) \times 2(N-1)} \quad (50)$$

$$\mathbb{M} = \begin{bmatrix} q_1 & 0 \\ 0 & 0 \end{bmatrix} \quad (51)$$

$$\mathbf{N} = [0 \quad (\sin\theta + \mu\cos\theta)m_2 g v_1 v_2 \quad \dots \quad 0 \quad (\sin\theta + \mu\cos\theta)m_N g v_1 v_N]_{1 \times 2(N-1)} \quad (52)$$

$$\mathbf{R} = r_1 \cdot \mathbf{I}_{N \times N} \quad (53)$$

$$\mathbf{D} = [q_2 m_1 v_1 \quad \dots \quad q_2 m_N v_N]_{1 \times N} \quad (54)$$

$$\mathbf{F} = \sum_{i=1}^N (m_i g \sin \theta + \mu m_i g \cos \theta) \cdot v_1 \quad (55)$$

Applying equation (5) and adding perturbation:

$$f(\mathbf{X}, \mathbf{U}) = \mathbf{A}\mathbf{X} + \mathbf{B}\mathbf{U} + \mathbf{C} \quad (56)$$

with

$$\mathbf{C} = [0 \quad \delta \quad \dots \quad 0 \quad \delta]^T_{2(N-1) \times 1} \quad (57)$$

where δ is a perturbation on the platoon leader's speed.

As the formulation of the proposed platoon controller is an optimal control problem, equation (47) indicates:

$$\frac{\partial \mathbf{H}}{\partial \mathbf{U}^*} = \mathbf{0} \quad (58)$$

By substituting equation (46) (49) (56) into equation (48) (57), the optimal control law of the proposed controller is as follows:

$$\mathbf{U}^* = -\mathbf{R}^{-1}(\mathbf{D}^T + \mathbf{B}^T \boldsymbol{\lambda}) \quad (59)$$

$$-\frac{d\boldsymbol{\lambda}}{dt} = \mathbf{M}\mathbf{X} + \mathbf{N}^T + \mathbf{A}^T \boldsymbol{\lambda} \quad (60)$$

Since string stability is better analyzed in frequency domain, Laplace transform is adopted:

Definition 2 (Laplace transform): Function $g(x)$ with $x \geq 0$ can be transformed into frequency domain as follows:

$$G(s) = \mathcal{L}\{g(x)\} = \int_0^{\infty} g(x)e^{-sx} dx \quad (61)$$

$$s \stackrel{\text{def}}{=} \iota\omega \quad (\omega \in \mathbb{R}^+) \quad (62)$$

where e denotes the natural logarithm, ι denotes imaginary number, and ω denotes angular speed in Laplace domain.

By applying Definition 2, $\mathbf{X}(x)$, $\mathbf{U}(x)$, and $\boldsymbol{\lambda}(x)$ are transformed into frequency domain as follows:

$$\boldsymbol{\chi}(s) \stackrel{\text{def}}{=} \mathcal{L}\{\mathbf{X}(x)\} \quad (63)$$

$$\mathbf{u}(s) \stackrel{\text{def}}{=} \mathcal{L}\{\mathbf{U}(x)\} \quad (64)$$

$$\mathbf{r}(s) \stackrel{\text{def}}{=} \mathcal{L}\{\boldsymbol{\lambda}(x)\} \quad (65)$$

By applying Definition 2 and equation (63) (64) (65), equation (56) (59) (60) are transformed into frequency domain as follows:

$$\boldsymbol{\chi} = (s\mathbf{I} - \mathbf{A})^{-1}(\mathbf{B}\mathbf{u} + \mathbf{C}) \quad (66)$$

$$\mathbf{u} = -\mathbf{R}^{-1}(\mathbf{D}^T + \mathbf{B}^T \mathbf{r}) \quad (67)$$

$$\mathbf{r} = -(s\mathbf{I} + \mathbf{A}^T)^{-1}(\mathbf{M}\boldsymbol{\chi} + \mathbf{N}^T) \quad (68)$$

Substituting equation (66) (68) into (67):

$$\mathbf{U} = (\mathbf{PMTB} - \mathbf{R})^{-1}(\mathbf{D}^T - \mathbf{PN}^T - \mathbf{PMT C}) \quad (69)$$

with

$$\mathbf{P} = \mathbf{B}^T (\mathbf{sI} + \mathbf{A}^T)^{-1} \quad (70)$$

$$\mathbf{T} = (\mathbf{sI} - \mathbf{A})^{-1} \quad (71)$$

Definition 3: Considering a platoon with one leader and $N - 1$ followers, the platoon is string stable if and only if:

$$\Gamma_{N,j,j-1} \stackrel{\text{def}}{=} \frac{\|\Delta a_j(s)\|_2}{\|\Delta a_{j-1}(s)\|_2} \leq 1, \forall j \in [2, N] \quad (72)$$

where $\Gamma_{N,j,j-1}$ is the acceleration oscillation transfer function between follower $j - 1$ and j in a platoon with N vehicles. $\Delta a_j(s)$ is the derivative of the i^{th} vehicle's acceleration with respect to perturbation, with $\Delta a_j(s) = \frac{\partial a_j(s)}{\partial \delta}$.

Substituting equation (8) (50) (52) (53) (54) (57) (70) (71) into (69), and assuming that: i) q_1, q_2 and r_1 have the same order of magnitude, ii) any v_i ($\forall i \in [1, N]$) has the same order of magnitude, iii) any m_i ($\forall i \in [1, N]$) has the same order of magnitude, the following equation can be calculated:

$$\Gamma_{N,j,1} = \frac{\|\Delta a_j(s)\|_2}{\|\Delta a_1(s)\|_2} = \left\| \frac{1}{N-1} \right\|_2 < 1, \forall j \in [2, N] \quad (73)$$

The stability criteria in Definition is satisfied. Therefore, the platoon under the proposed Eco-CACC is string stable regardless of platoon size. This concludes the proof. ■

V. EVALUATION

The effectiveness of the proposed Eco-CACC system has undergone comprehensive evaluation. The assessments are categorized as follows: (i) an examination of platoon's fuel efficiency on rolling terrains, (ii) an evaluation of platoon's stability, and (iii) a measurement of controller's computational efficiency.

A. Experiment Design

1) Test bed

A MATLAB-based simulation platform serves as the test bed. An 800-meter-long straight road with four undulating slopes is simulated to mimic hilly terrain.

2) Scenario design

The scenario involves a platoon of three vehicles navigating this hilly road, with the objective to minimize total fuel consumption while maintaining a specified time gap between vehicles. The slope of the hilly road is designed as shown in Figure 2.

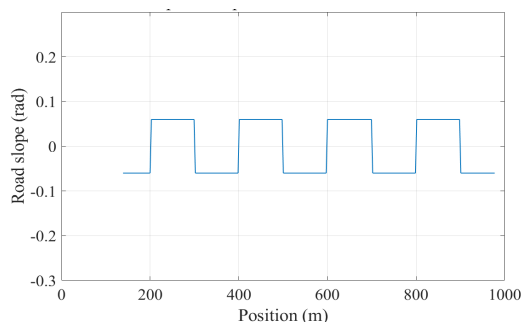


Figure 2. Road slope along driving positions

3) Sensitivity analysis

This analysis examines the adaptability of the proposed Eco-CACC system to different road types:

- Major arterial: The target speed is set at 65 mph, with a maximum slope intensity of 6%.
- Collector road: The target speed is set at 45 mph, with a maximum slope intensity of 15%.

The slope assigned to each road type is in accordance with the guideline from the "Green Book" (Hancock M W et al., 2013).

4) Controller types

Two distinct controller paradigms are subjected to evaluation:

- Traditional CACC controller: The traditional CACC controller is previously developed by the research team (Zhang Y et al., 2022). This controller's primary objective is to maintain a minimal and constant inter-vehicular distance. However, it lacks the capability to respond to changing road slopes, rendering it static with respect to the topographical variability. The platoon adopting the traditional CACC controller is defined as CACC platoon.
- The proposed Eco-CACC controller: This proposed controller is designed with the explicit capability to account for variable road slopes, particularly suited for rolling terrains. Furthermore, it incorporates an optimization algorithm that seeks to minimize the energy consumption of each vehicle individually, thereby promoting an enhanced level of global optimality across the platoon. The platoon adopting the proposed Eco-CACC controller is defined as Eco-CACC platoon.

5) Parameter settings

The parameters in the proposed Eco-CACC controller are set as follows.

Table 1. Parameter Settings

Parameter	Explanation	Default value	Units
Δs	Space increment	0.1	meter
v_{max}	Speed limit	75	mph
$a_{i,max}$	Maximum acceleration of the i^{th} vehicle	3	m/s ²
$a_{i,min}$	Minimum acceleration of the i^{th} vehicle	-5	m/s ²
h	Expected time headway	1	second
q_1	Weighting parameter for CACC cost	500	/
q_2	Weighting parameter for ecology cost	10	/
q_3	Weighting parameter for terminal cost	5000	/
m_i	Mass of the i^{th} vehicle	1400	kg
g	Gravity	9.8	m/s ²
μ	Constant describing the rolling resistance	0.015	/
ξ	Constant describing drag	0.000024	kg/m

6) Measurements of effectiveness

Measurements of Effectiveness (MOEs) are categorized as follows:

- Platoon's fuel efficiency: Fuel efficiency is quantified by the accumulated fuel consumption. It is calculated by a VT-micro model (H. Rakha, 2004).
- Platoon's stability: Platoon stability is evaluated by the longitudinal following errors within a platoon. It is calculated by $t_{1,k} - t_{i,k} - (i - 1)h$ in equation (2).

- Computational efficiency: Computational efficiency is quantified by the computation time for an execution of the proposed Eco-CACC controller.

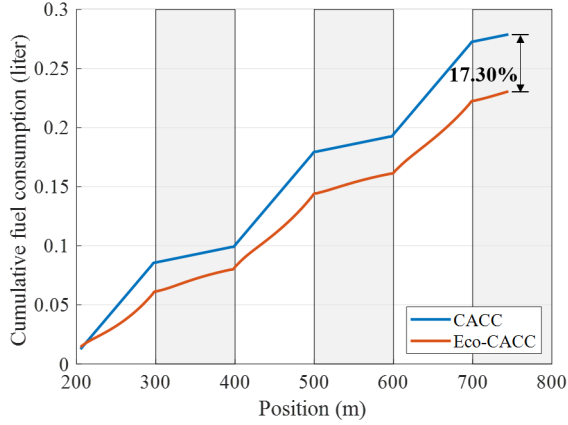
B. Results

The experimental findings validate the capabilities of the proposed Eco-CACC controller, showcasing its ability to: i) improve platoon's fuel efficiency on rolling terrains by 17.30%~37.67%, ii) ensure platoon's stability, and iii) maintain an average computation time within 55 milliseconds.

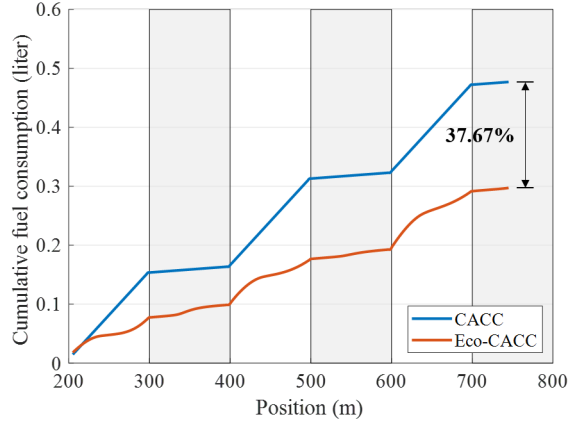
1) Platoon's fuel efficiency

The proposed Eco-CACC controller is capable of enhancing the platoon's fuel efficiency by 17.30% on major arterials and 37.67% on collector roads. This superiority is depicted in Figure 3, illustrating the cumulative fuel consumption of both the Eco-CACC platoon and the baseline CACC platoon. Furthermore, the ecological benefit of the proposed Eco-CACC controller exhibits an expanding trend with increasing travelling distance. This finding reinforces the sustainable advantage of the proposed Eco-CACC system in large-scale applications.

Figure 3 further reveals that the ecological benefit of the proposed Eco-CACC controller is particularly obvious during uphill travel. It is confirmed by the greater disparity between Eco-CACC platoon and CAC platoon during uphill travel (with a white background) compared to downhill travel (with a gray background). This effect is attributed to that Eco-CACC platoon could overcome resistance during uphill by harnessing the kinetic energy accumulated during downhill, without consuming extra fuel energy.



(a) At major arterial

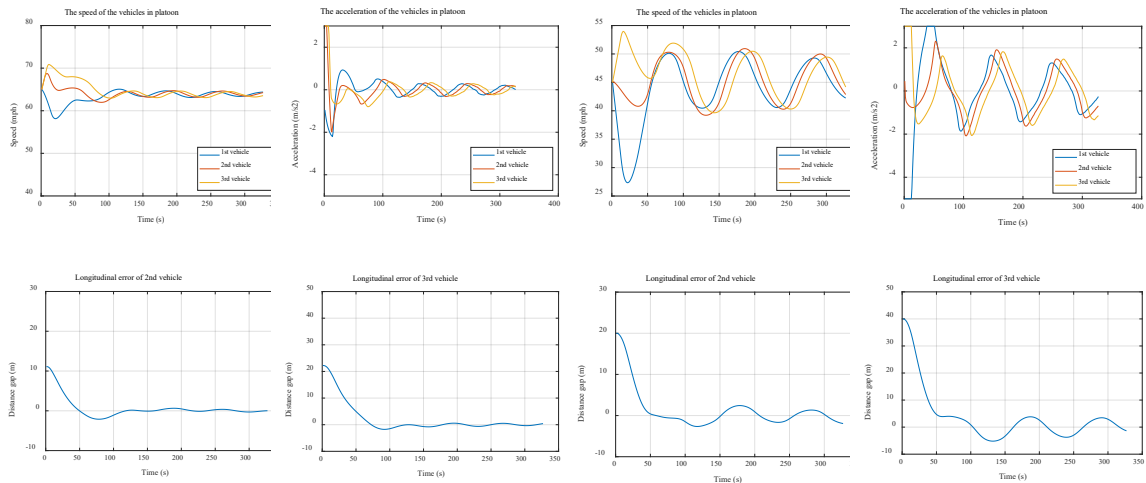


(b) At collector road

Figure 3. Cumulative fuel consumption of Eco-CACC and CACC

2) *Platoon's stability*

The proposed Eco-CACC controller is capable of guaranteeing the platoon's stability. It is confirmed by the longitudinal following errors, as shown in Figure 4. Figure 4 demonstrates a sample case of Eco-CACC platoon on both major arterial and collector road. It highlights that the longitudinal errors of the followers in the platoon diminish along full up-down slopes. Eco-CACC platoon has the ability to maintain a stable spacing.



(a) At major arterial

(b) At collector road

Figure 4. Trajectories of the Eco-CACC platoon (a sample case)

3) Computational efficiency

Despite its effective performance, the proposed Eco-CACC controller can still guarantee computational efficiency. It is confirmed by the computation time for an execution of the controller, as shown in Figure 5. It is demonstrated that the computation time is less than 96 milliseconds over various control steps and control horizons. The average computation time is just 55 milliseconds, showcasing the online implementation capability of the controller.

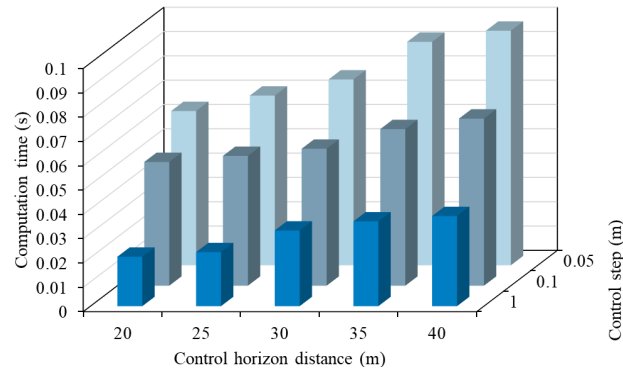


Figure 5. The computation time for an execution of the proposed Eco-CACC controller

VI. DISCUSSION

According to the performances of the proposed Eco-CACC system in the experiments, both mobility and fuel efficiency improvement can be achieved when applying the proposed Eco-CACC system to road transportation. The mobility improvement is born by trajectory optimization coordinating the states of the vehicles in the platoon. The fuel efficiency improvement is born by trajectory optimization coordinating road slopes. Furthermore, when transportation managers give priority to mobility, the weight of cooperative cruising

in the objective function of the proposed Eco-CACC controller shall be increased. When transportation managers give priority to fuel efficiency, the weight of reducing fuel consumption in the objective function of the proposed Eco-CACC controller shall be increased.

VII. CONCLUSION

This paper proposes a nonlinear optimal control based Eco-CACC controller. It has the following features: i) enhancing performance across rolling terrains by modeling in space domain; ii) enhancing fuel efficiency via globally optimizing all vehicle's fuel consumptions; iii) ensuring computational efficiency by developing a differential dynamic programming-based solving method for the non-linear optimal control problem; iv) ensuring string stability through theoretically proving and experimentally validating.

The performance of the proposed Eco-CACC controller was evaluated. The influence of different road types on the performance was analyzed. Experiment results showed that applying the proposed system can improve fuel economy while guaranteeing the effectiveness of platooning. Detailed investigation on the results reveals that:

- The proposed Eco-CACC controller brings significant benefit in fuel efficiency. The average fuel saving is about 37.67% on collector road and about 17.30% at major arterial.
- The fuel-saving benefit is more obvious when the ego vehicle is going uphill.
- The proposed Eco-CACC controller improves fuel efficiency while maintaining a stable spacing compared to a traditional CACC controller.

However, the proposed controller does not involve lateral control. Further work could consider coupling longitudinal and lateral control. The enhancement would further improve the performance of the platoon.

ACKNOWLEDGMENT

This paper is partially supported by National Key R&D Program of China (No. 2022YFF0604905), National Natural Science Foundation of China (No. 52302412 and 52372317), Shanghai Automotive Industry Science and Technology Development Foundation (No. 2213), Tongji Zhongte Chair Professor Foundation (No. 000000375-2018082), Shanghai Sailing Program (No. 23YF1449600), Shanghai Post-doctoral Excellence Program (No.2022571), China Postdoctoral Science Foundation (No.2022M722405), and the Science Fund of State Key Laboratory of Advanced Design and Manufacturing Technology for Vehicle (No. 32215011).

REFERENCES

- Bellman, R. (1966). Dynamic programming. *science*, 153(3731), 34-37.
- Duan, H., Gao, X., Wang, J., Liu, X., & Sun, G. (2022, October). Study of cooperative adaptive cruise control system based on model predictive control. In *2022 IEEE 4th International Conference on Civil Aviation Safety and Information Technology (ICCASIT)* (pp. 201-207). IEEE.
- Han, S. Y., Chen, Y. H., Wang, L., & Abraham, A. (2013, October). Decentralized longitudinal tracking control for cooperative adaptive cruise control systems in a platoon. In *2013 IEEE International Conference on Systems, Man, and Cybernetics*. IEEE.
- Hancock, M. W., & Wright, B. (2013). A policy on geometric design of highways and streets. *American Association of State Highway and Transportation Officials: Washington, DC, USA*, 3.

- Kazemi, H., Mahjoub, H. N., Tahmasbi-Sarvestani, A., & Fallah, Y. P. (2018). A learning-based stochastic MPC design for cooperative adaptive cruise control to handle interfering vehicles. *IEEE Transactions on Intelligent Vehicles*, 3(3), 266-275.
- Li, J., Chen, C., Yang, B., He, J., & Guan, X. (2023). Energy-Efficient Cooperative Adaptive Cruise Control for Electric Vehicle Platooning. *IEEE Transactions on Intelligent Transportation Systems*.
- Lin, Y. C., & Nguyen, H. L. T. (2019). Adaptive neuro-fuzzy predictor-based control for cooperative adaptive cruise control system. *IEEE Transactions on Intelligent Transportation Systems*, 21(3), 1054-1063.
- Liu, B., & El Kamel, A. (2015). V2X-based decentralized cooperative adaptive cruise control in the vicinity of intersections. *IEEE Transactions on Intelligent Transportation Systems*, 17(3), 644-658.
- Luu, D. L., Pham, H. T., Lupu, C., Nguyen, T. B., & Ha, S. T. (2021, August). Research on cooperative adaptive cruise control system for autonomous vehicles based on distributed model predictive control. In *2021 International Conference on System Science and Engineering (ICSSE)* (pp. 13-18). IEEE.
- Ma, H., Chu, L., Guo, J., Wang, J., & Guo, C. (2020). Cooperative adaptive cruise control strategy optimization for electric vehicles based on SA-PSO with model predictive control. *IEEE Access*, 8, 225745-225756.
- Murgovski, N., Egardt, B., & Nilsson, M. (2016). Cooperative energy management of automated vehicles. *Control Engineering Practice*, 57, 84-98.
- Nocedal, J., & Wright, S. J. (Eds.). (1999). *Numerical optimization*. New York, NY: Springer New York.
- Rajamani, R. (2011). *Vehicle dynamics and control*. Springer Science & Business Media.
- Rakha, H., Ahn, K., & Trani, A. (2004). Development of VT-Micro model for estimating hot stabilized light duty vehicle and truck emissions. *Transportation Research Part D: Transport and Environment*, 9(1), 49-74.
- Rezaee, H., Parisini, T., & Polycarpou, M. M. (2023). Leaderless Cooperative Adaptive Cruise Control Based on Constant Time-Gap Spacing Policy. *IEEE Transactions on Automatic Control*.
- Sakhdari, B., & Azad, N. L. (2017). A distributed reference governor approach to ecological cooperative adaptive cruise control. *IEEE Transactions on Intelligent Transportation Systems*, 19(5), 1496-1507.

- Wang, H., Lai, J., Zhang, X., Zhou, Y., Li, S., & Hu, J. (2022). Make space to change lane: A cooperative adaptive cruise control lane change controller. *Transportation research part C: emerging technologies*, 143, 103847.
- Turri, V., Besselink, B., & Johansson, K. H. (2016). Cooperative look-ahead control for fuel-efficient and safe heavy-duty vehicle platooning. *IEEE Transactions on Control Systems Technology*, 25(1), 12-28.
- Turri, V., Flårdh, O., Mårtensson, J., & Johansson, K. H. (2018, June). Fuel-optimal look-ahead adaptive cruise control for heavy-duty vehicles. In *2018 Annual American Control Conference (ACC)* (pp. 1841-1848). IEEE.
- Wang, Z., Wu, G., & Barth, M. J. (2018, November). A review on cooperative adaptive cruise control (CACC) systems: Architectures, controls, and applications. In *2018 21st International Conference on Intelligent Transportation Systems (ITSC)* (pp. 2884-2891). IEEE.
- Wang, Z., Wu, G., Hao, P., Boriboonsomsin, K., & Barth, M. (2017, June). Developing a platoon-wide eco-cooperative adaptive cruise control (CACC) system. In *2017 IEEE Intelligent Vehicles Symposium (IV)* (pp. 1256-1261). IEEE.
- Zhai, C., Luo, F., Liu, Y., & Chen, Z. (2018). Ecological cooperative look-ahead control for automated vehicles travelling on freeways with varying slopes. *IEEE Transactions on Vehicular Technology*, 68(2), 1208-1221.
- Zhang, Y., Bai, Y., Wang, M., & Hu, J. (2020). Cooperative adaptive cruise control with robustness against communication delay: An approach in the space domain. *IEEE Transactions on Intelligent Transportation Systems*, 22(9), 5496-5507.
- Zhang, Y., Wu, Z., Zhang, Y., Shang, Z., Wang, P., Zou, Q., ... & Hu, J. (2022). Human-lead-platooning cooperative adaptive cruise control. *IEEE Transactions on Intelligent Transportation Systems*, 23(10), 18253-18272.